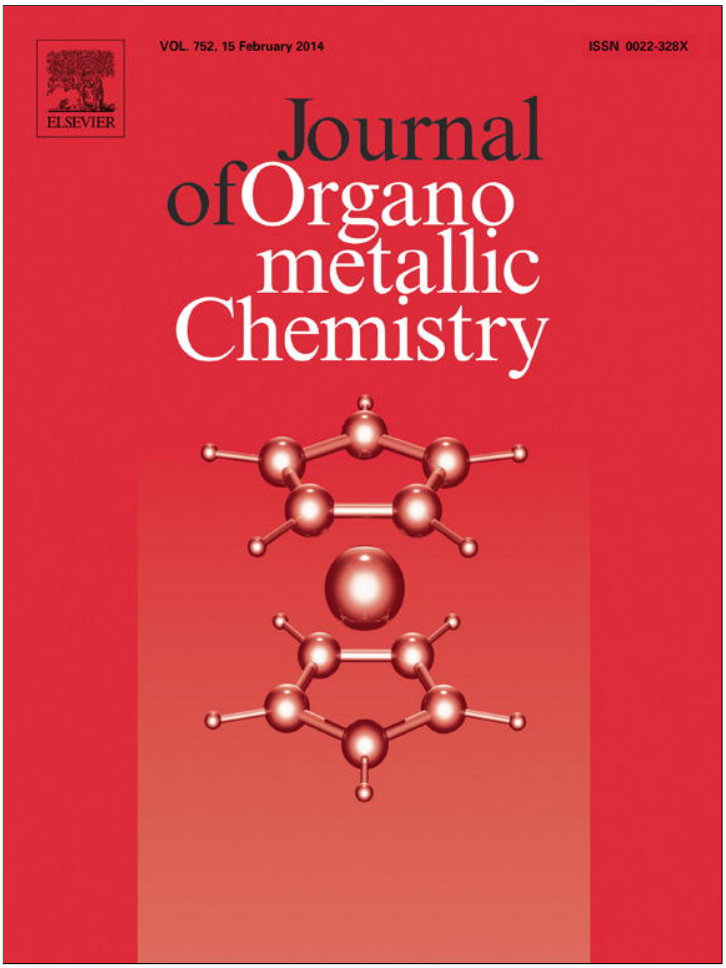

Journal of Organometallic Chemistry 752 (2014) 152–160

Contents lists available at ScienceDirect

Journal of Organometallic Chemistry

journal homepage: www.elsevier.com/locate/jorganchem

Structural and theoretical studies of mono and di-insertion of symmetric alkynes into the Pd–C σ bond of cyclopalladated secondary (*tert*-butyl and ethyl) benzylamines

Kazem Karami [a,*], Mahboubeh Hosseini-Kharat [a], Corrado Rizzoli [b], Hossein Tavakol [a], Janusz Lipkowski [c]

[a] Department of Chemistry, Isfahan University of Technology, Isfahan 84156/83111, Iran
[b] Department of Chemistry, University of Parma, I-43124 Parma, Italy
[c] Institute of Physical Chemistry, Polish Academy of Sciences, Kasprzaka 44/52, 01-224 Warsaw, Poland

ARTICLE INFO

Article history:
Received 22 August 2013
Received in revised form
12 November 2013
Accepted 16 November 2013

Keywords:
Cyclopalladated complex
Insertion reaction
DMAD
Diphenylacetylene
Theoretical study

ABSTRACT

The reactivity of the dinuclear cyclopalladated complexes derived from secondary benzylamines, $[Pd_2\{(C,N)-C_6H_4CH_2NH(R)\}_2(\mu\text{-}X)_2]$ [X = Br, R = *t*-Bu (**1a**); X = Cl, R = *t*-Bu (**1b**); X = Cl, R = Et (**1c**)] is reported. **1a** reacted with dimethyl acetylenedicarboxylate (DMAD) to yield the mono-inserted complex $[Pd_2\{(C,N)-C(CO_2Me)=C(CO_2Me)C_6H_4CH_2NH(t\text{-}Bu)\}_2(\mu\text{-}Br)_2]$ (**2a**). **1a**, **1b** and **1c** reacted with (R′)C≡C(R′) (R′ = CO_2Me, Ph) to give $[Pd\{(C,N)\ C(R')=C(R')C(R')=C(R')C_6H_4CH_2NH(R)\}X]$ [X = Br, R = *t*-Bu, R′ = CO_2Me (**3a**); X = Cl, R = *t*-Bu, R′ = Ph (**2b**); X = Cl, R = Et, R′ = Ph (**2c**)] through a double insertion of the alkyne into the Pd–C σ bond. **2c** also reacts with $Ag(CF_3SO_3)$ and pyridine to give mononuclear cationic complex $[Pd\{(C,N)-C(Ph)=C(Ph)C(Ph)=C(Ph)\}C_6H_4CH_2NH(Et)(py)]CF_3SO_3$ (**3c**). The crystal structures of di-inserted complexes **2b**, **2c** and **3c** have been determined by X-ray diffraction studies. Their molecular structures showed that the conformation of the C=C double bonds within the butadienyl group attached to the aromatic ring was *trans–cis*. Density functional theory (DFT) calculations also indicated that this arrangement is more stable than other possible conformations.

1. Introduction

The insertion of alkynes into the Pd–C bond of cyclopalladated complexes has received great attention. In some cases the palladation reaction and the insertion of the alkyne form part of a catalytic cycle yielding interesting organic compounds [1–17]. Most reactions of palladacycles with alkynes give stable complexes because of intramolecular stabilization of the coordinated atom. However, sometimes the resulting cyclopalladated complex is unstable and gives interesting organic products [18,19] or a non-cyclopalladated aryl palladium complex forms a stable cyclopalladated derivative after the insertion of the alkyne [20].

It is well known that the nature of the final product formed by the insertion of alkynes depends on a wide variety of factors including the nature of the metalated carbon, the electron-withdrawing or -donating ability of the substituents on the alkyne, the stoichiometry of the reaction, the remaining ligands bound to the palladium, etc [20–23]. In this context, the reaction between internal alkynes with electron-withdrawing substituents and cyclometalladated compounds favors the production of mono-inserted products, while internal alkynes with electron-donating substituents promotes the synthesis of di-inserted products [24]. The mechanism of these insertion reactions show that mono-inserted derivatives are difficult to prepare if the rate of the second insertion is much greater than the first one [25].

Recently, a number of N-ligand derivatives have found practical applications and the search for new, more useful and/or selective species is still in progress [26]. N-containing palladacycles are the most common palladacycles that undergo alkyne insertion because these compounds are much more reactive than the corresponding palladacycles where the heteroatom is phosphorus or sulfur [27]. Insertion of one, two or three molecules of the alkyne into the Pd–C bond of amine palladacycles has been reported [7,8,22–24,28–37]. Although the insertion reactions of alkynes into cyclopalladated primary amines are well-known [38], this is not so for secondary amines.

The first study of the reactivity of a cyclopalladated secondary amine with alkynes, was reported by Vicente et al. [30] in which

* Corresponding author. Tel.: +98 3113913239; fax: +98 3113912350.
E-mail addresses: karami@cc.iut.ac.ir (K. Karami), m.hosseinikharat@ch.iut.ac.ir (M. Hosseini-Kharat).

0022-328X/$ – see front matter © 2013 Elsevier B.V. All rights reserved.
http://dx.doi.org/10.1016/j.jorganchem.2013.11.030

insertion of two molecules of alkynes occurred into the Pd–C bond of the dimeric starting complex. In other attempts they tried to obtain di-inserted derivatives from six-membered ortho-metalated secondary amine and 2-butyne, 3-hexyne, or diphenylacetylene, but it was unsuccessful due to the formation of an unstable 10-membered vinyl-palladated ring [34]. In this paper, regarding to the fact that articles focusing on the reactivity of the Pd–C σ bond of secondary amine cyclopalladated complexes are not so common and also a few crystal structures of them have been reported in the literature, we have used two symmetric alkynes, which expand a five-membered secondary amine palladacycles **1a**–**1c** to a seven and nine-membered palladacycles by insertion of one and two molecules of alkynes into the Pd–C σ bonds. To the best of our knowledge, the present work is the first reporting of the crystal structures of the neutral complexes (**2b** and **2c**) from di-insertion of two molecules of alkyne (diphenylacetylene) into the Pd–C bond of cyclopalladated secondary amines. Furthermore, we report the crystal structure of new cationic mononuclear organopalladium complex (**3c**) which is formed by the reaction of neutral di-inserted complex (**2c**) with the pyridine ligand. Theoretical studies using density functional theory (DFT) calculations, have also been carried out in order to investigate the influence of the nature of the substituents in the alkynes on the LUMO–HOMO energy gap of the di-inserted products, and obtain molecular parameters and partial atomic charges around the created nine-membered cycle so as to compare relative energies of possible conformations of the C=C double bonds within the butadienyl fragment of the di-inserted complexes.

2. Results and discussion

2.1. Synthesis and spectroscopic characterization

We have previously described the formation of five-membered acetato-bridged dinuclear palladacycles of general formula [Pd(benzylamine)(μ-OAc)]$_2$ from the reaction of the secondary benzylamines PhCH$_2$NH(Et) or PhCH$_2$NH(*t*-Bu) with Pd(OAc)$_2$ [39]. Treatment of acetato-bridged complexes with an excess of NaCl or NaBr in methanol afforded the corresponding chloro- and bromo-bridging dimers **1a**–**1c** [39,40]. In order to prepare mono- and di-inserted complexes, reactions of the **1a**–**1c** with two symmetric alkynes were studied. Under the reaction conditions, **1a** and **1c** reacted with MeO$_2$CC≡CCO$_2$Me (1:2 and 1:4 M ratio for mono and di-insertion, respectively). Reaction of **1c** with MeO$_2$CC≡CCO$_2$Me gave complicated mixtures that were not separable, but the reaction of **1a** afforded complexes **2a** and **3a**, resulting from the insertion of one and two molecule of alkyne into the Pd–aryl bond (Scheme 1). Formation of **2a** is remarkable considering that, mono-inserted products are not common. We can relate the difference in reactivity of **1a** and **1c** with MeO$_2$CC≡CCO$_2$Me to the greater basic character of complex **1a** which lead to the more stable insertion products [29]. In the IR spectra of **2a** and **3a** two bands in the range 3060–3250 cm^{-1} were assigned to the NH stretching of the amino groups. In addition, the IR spectra show two strong peaks at 1709, 1628 and four very strong peaks at 1725, 1713, 1690 and 1670 cm^{-1} corresponding to ν(CO$_2$) [29], suggesting that mono and di-insertion products were obtained. In the ^{1}H NMR spectra of **2a**

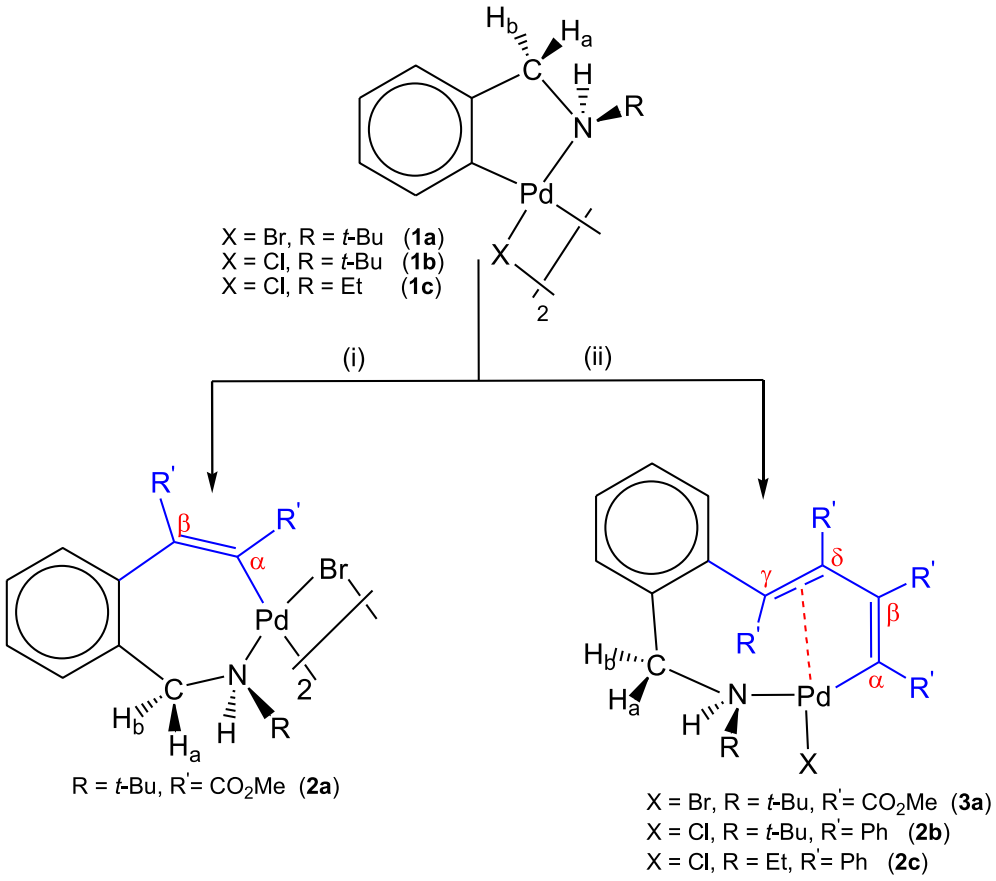

Scheme 1. (i) MeO$_2$CC≡CCO$_2$Me, acetone, room temperature, 6 h; (ii) alkyne, acetone, reflux, 3 h (complex **3a**). Alkyne, dichloromethane, room temperature, 6 h (complex **2b** and **2c**).

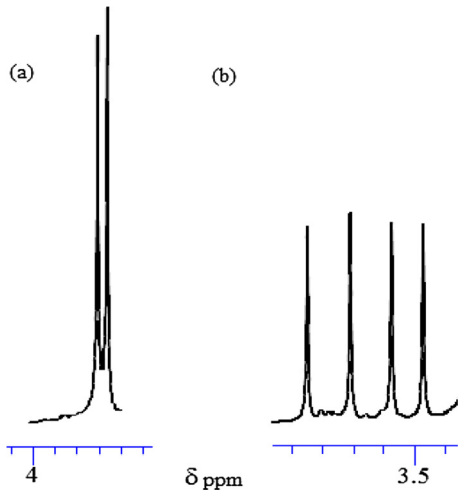

Fig. 1. Methoxy region of the ^{1}H NMR spectra of mono-inserted complex **2a** (a) and di-inserted complex **3a** (b).

and **3a**, the NH protons and the *tert*-butyl protons appeared at δ 4.4 and 3.08 ppm as broad signals and at δ 1.35 and 1.46 ppm as sharp singlets, respectively. Methylene protons in **2a** and **3a** appeared as AB patterns, indicating that they are situated in different environments. But the most relevant features observed in the ^{1}H NMR spectra are the presence of two resonances at δ 3.65 and 3.69 ppm (**2a**) and four resonances at δ 3.46, 3.54, 3.65 and 3.76 ppm (**3a**), corresponding to different OMe groups (Fig. 1). Moreover these signals were observed at δ 51.0 and 52.0 ppm and δ 51.2, 51.3, 51.8, and 52.5 ppm in the ^{13}C{^{1}H} NMR spectra of **2a** and **3a**, respectively. The signals due to the two and four types of carbon nuclei of the ethylene (C^{α}–C^{β}) and butadienyl (C^{α}–C^{γ}) units appeared at δ 126.7 and 151.6 ppm and δ 126.1, 135.3, 143.4 and 155.0 ppm, respectively, and exhibited low intensity [41]. In addition, the resonances corresponding to the CO carbon atoms (δ 166.3 and 167.1 ppm for **2a**) and (δ 157.8, 165.1, 168.0 and 171.0 ppm for **3a**) of ester groups are within the expected range [34]. These data strongly support the hypothesis that mono- and di-insertion of $MeO_2CC{\equiv}CCO_2Me$ into the palladium–carbon bonds has occurred. Reaction of **1b** and **1c** with PhC≡CPh also afforded the nine-membered cyclopalladated complexes **2b** and **2c** which were obtained from the insertion of two molecules of alkyne into the Pd–C σ bond (Scheme 1). Attempts to gain the monoinsertion products of **1b** and **1c** in the reaction with PhC≡CPh were unsuccessful. A similar behavior has already been observed in the reaction of cyclopalladated primary and tertiary amines with PhC≡CPh [29,34]. It was reported that, with electron rich acetylenes like PhC≡CPh, the synthesis of the di-inserted complex, without isolation or observation of the mono-inserted intermediate can occurs mainly. Kinetic studies have shown that this is due to the fact that formation of the mono-inserted complex is the rate-determining step [25]. As previously mentioned in the introduction section, if the rate of the second insertion is greater than the first one, the preparation of the mono-inserted derivatives is difficult. Complexes **2b** and **2c** were obtained at room temperature in good yields, and no evidence of the formation of any other complex was detected by ^{1}H or ^{13}C{^{1}H} NMR. This finding suggests that the presence of the two phenyl rings on the alkyne might introduce significant steric effects which may hinder insertion of the second molecule of PhC≡CPh. According to mechanistic studies on alkyne insertions reported by Ryabov et al. [25], a *cis* → *trans* isomerization of the olefinic fragment (of the monoinsertion product) takes place during insertion of the second molecule of the alkyne. In the ^{1}H NMR spectra of **2b** and **2c**, similarly to the cases for **2a** and **3a**, the methylene protons are also nonequivalent and resonate at different places (δ 3.33 and 3.63 ppm) and (δ 2.33 and 4.57 ppm), respectively. In both complexes, signals due to the phenyl protons of the alkyne and the four aromatic protons of the benzyl moiety were overlapped with each other and appeared at (6.81–7.51 ppm for **2b**) and (6.55–7.83 ppm for **2c**). In the ^{13}C{^{1}H} NMR spectra of **2b** and **2c**, the resonances of the four types of carbon nuclei of the butadienyl units (C^{α}–C^{γ}) appeared at δ 141.6, 135.6, 134.3 and 124.8 ppm and δ 140.8, 135.8, 132.9 and 125.8 ppm, respectively, and also exhibited low intensity [41]. Complex **2c** reacts with $Ag(CF_3SO_3)$ and pyridine to give cationic complex **3c** (Scheme 2). The IR spectrum of **3c** shows a number of strong absorptions at 1260–1000 cm^{-1} due to the presence of an uncoordinated $CF_3SO_3^-$ anion. The bands at 1257 and 1029 cm^{-1} are assigned to the asymmetric and symmetric vibration of the SO_3 fragment respectively and the 1159 cm^{-1} band is related to the symmetric CF_3 vibrational mode [42–44].

The ^{1}H and ^{13}C{^{1}H} NMR spectra of **3c** show similar patterns to those in **2b** and **2c**. However, in **3c**, signals due to the pyridine ligand are observed, and in its ^{1}H NMR spectrum, one of the *ortho*-protons of pyridine is significantly shifted to higher frequency (9.48 ppm, $^3J_{HH}$ = 6.4 Hz).

2.2. Single crystal X-ray diffraction studies

The molecular structures of **2b**, **2c** and **3c** were determined by X-ray diffraction studies. The X-ray molecular structures and selected bond lengths and bond angles are shown in Figs. 2–4, respectively. The crystal data and structural refinement parameters are listed in Table 1. In complexes **2b** and **2c**, the palladium atom is effectively four-coordinated, since it is bound to a chloro ligand, the nitrogen atom, the terminal carbon atom C11 or C7 of the η^3-butadienyl fragment, and the mid-point of the C8=C9 or C4=C5 double bond in

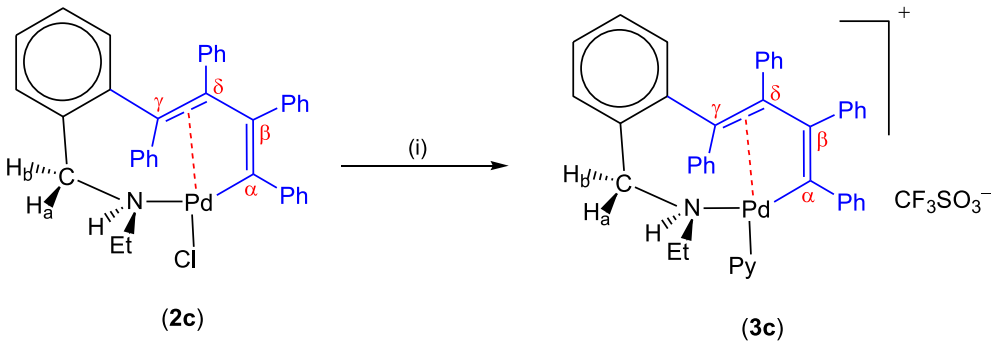

Scheme 2. (i) $Ag(CF_3SO_3)$, acetone, pyridine, r.t.

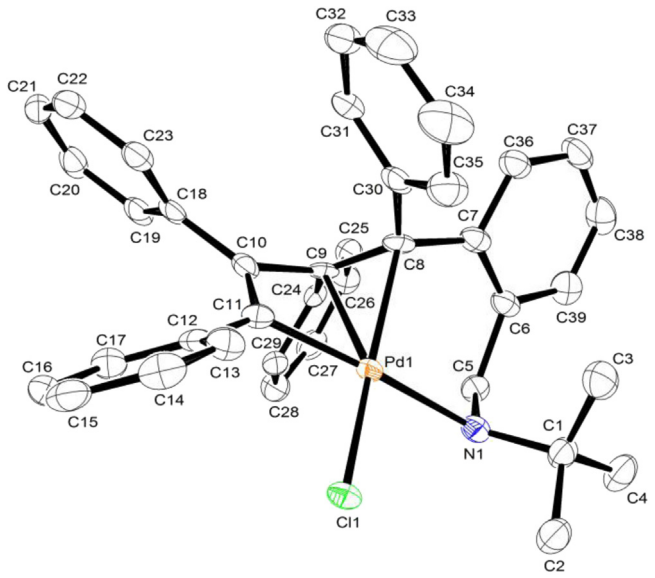

Fig. 2. ORTEP diagram for palladacycle **2b** with ellipsoids drawn at the 70% probability level. The hydrogen atoms have been omitted for clarity. Selected bond lengths (Å) and angles (°): Pd1–Cl1 2.3305(8), Pd1–N1 2.228(3), Pd1–C11 1.997(3), Pd1–C9 2.227(3), Pd1–C8 2.210(3), N1–C5 1.481(4), C5–C6 1.513(4), C6–C7 1.406(5), C7–C8 1.507(5), C8–C9 1.419(5), C9–C10 1.514(4), C10–C11 1.335(5), Cl1–Pd1–N1 92.67(7), Cl1–Pd1–C9 150.29(8), Cl1–Pd1–C8 165.84(8), Cl1–Pd1–C11 91.80(9), N1–Pd1–C11 167.93(11), N1–Pd1–C9 106.61(11), N1–Pd1–C8 93.59(11), C11–Pd1–C9 65.16(12), C11–Pd1–C8 84.63(12), Pd1–N1–C5 106.05(19), N1–C5–C6 113.8(3), C5–C6–C7 124.2(3), C6–C7–C8 125.2(3), C7–C8–C9 122.3(3), C8–C9–C10 117.0(3), C9–C10–C11 106.3(3), C10–C11–Pd1 48.46(17).

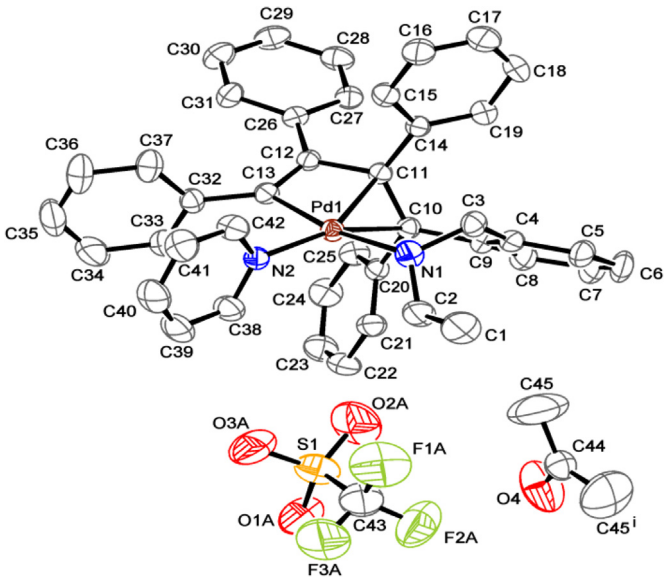

Fig. 4. ORTEP diagram for palladacycle **3c** with ellipsoids drawn at the 30% probability level. The hydrogen atoms have been omitted for clarity. Selected bond lengths (Å) and angles (°): Pd1–N2 2.014(3), Pd1–N1 2.156(3), Pd1–C13 1.985(4), Pd1–C11 2.140(3), Pd1–C10 2.189(4), N1–C3 1.446(5), C3–C4 1.507(6), C4–C9 1.396(6), C9–C10 1.514(5), C10–C11 1.395(5), C11–C12 1.504(5), C12–C13 1.289(5), N2–Pd1–N1 91.08(13), N2–Pd1–C11 155.64(14), N2–Pd1–C10 160.69(14), N2–Pd1–C13 92.73(14), N1–Pd1–C13 169.15(15), N1–Pd1–C11 107.49(14), N1–Pd1–C10 92.30(14), C13–Pd1–C11 66.29(14), C13–Pd1–C10 87.45(14), Pd1–N1–C3 112.7(2), N1–C3–C4 114.1(4), C3–C4–C9 124.6(4), C4–C9–C10 126.3(4), C9–C10–C11 122.7(3), C10–C11–C12 119.8(3), C11–C12–C13 107.8(3), C12–C13–Pd1 99.3(3).

2b and **2c**, respectively. The deviation of the metal from the mean planes formed by Cl1, C11, N1, C8 and C9 for **2b** and Cl1, C7, N1, C4 and C5 for **2c** is 0.124(2) Å and 0.042(2) Å, respectively. The first alkyne fragment inserted as a *trans* group π-bonded to palladium, while the

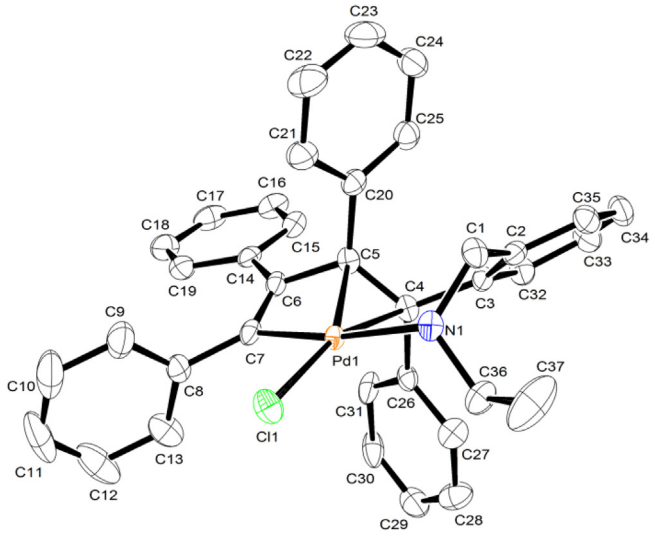

Fig. 3. ORTEP diagram for palladacycle **2c** with ellipsoids drawn at the 70% probability level. The hydrogen atoms have been omitted for clarity. Selected bond lengths (Å) and angles (°): Pd1–Cl1 2.3169(4), Pd1–N1 2.1534(14), Pd1–C7 2.0111(16), Pd1–C5 2.1972(15), Pd1–C4 2.2106(16), N1–C1 1.477(2), C1–C2 1.507(2), C2–C3 1.403(2), C3–C4 1.512(2), C4–C5 1.403(2), C5–C6 1.508(2), C6–C7 1.333(2), Cl1–Pd1–N1 86.77(4), Cl1–Pd1–C5 157.34(4), Cl1–Pd1–C4 163.39(5), Cl1–Pd1–C7 96.64(5), N1–Pd1–C7 172.02(6), N1–Pd1–C5 109.74(6), N1–Pd1–C4 90.25(6), C7–Pd1–C5 65.11(6), C7–Pd1–C4 88.48(6), Pd1–N1–C1 112.67(10), N1–C1–C2 114.54(13), C1–C2–C3 124.86(14), C2–C3–C4 127.37(14), C3–C4–C5 118.70(14), C4–C5–C6 121.13(14), C5–C6–C7 105.88(14), C6–C7–Pd1 48.90(9).

second one is *cis*, with the C7 or C11 carbon atom σ-bonded to palladium and *trans* coordinated to the amine N atom. As expected, the carbon–carbon distances of the alkene units coordinated η^2 to the palladium(II) are larger than those of the alkene units coordinated κ^1 to the palladium(II): 1.419(5) and 1.335(5) Å for **2b** and 1.403(2) and 1.333(2) Å for **2c**. Also the alkene unit with an η^2 coordination mode in **2b** does not deviate very much from planarity [torsion angle C7–C8–C9–C10 = −175.3(3)°] in relation to that in **2c** [torsion angle C3–C4–C5–C6 = 171.48(14)°]. The complexes adopt the structure found in most organopalladium complexes derived from the insertion of two alkyne molecules into the Pd–C σ bonds of five- and six-membered cyclopalladated complexes [29,32,33,41,45,46]. The Pd–Cl distances (2.3305(8) Å for **2b** and 2.3169(4) Å for **2c**) and the Pd–N distances (2.228(3) Å for **2b** and 2.1534(14) Å for **2c**) are shorter and longer, respectively, than the analogous distances in related cyclopalladated complexes of general formula *trans-N,P*-[Pd(*C,N*)Cl(phosphine)] [47–50]. This is due to the weaker *trans* influence of an η^2-coordinated alkene compared to a metalated carbon atom and to the stronger *trans* influence of a metalated carbon atom with respect to a phosphine ligand [51]. In both complexes, bond lengths and angles around the palladium(II) center are within the normal range for this kind of organopalladium complexes [52–54]. The C8–C9 (1.419(5) Å) and C4–C5 (1.403(2) Å) bond distances are slightly longer than the C10–C11 (1.335(5) Å) and C6–C7 (1.333(2) Å) bond distances for **2b** and **2c**, respectively, due to coordination to the palladium atom. Comparing **2b** and **2c**, the Pd1–N1 distance (2.228(3) Å) for **2b** is longer than the Pd1–N1 distance (2.1534(14) Å) for **2c**. Considering that the *tert*-butyl group in **2b** is bulkier than the ethyl group in **2c**, therefore, the sterically demanding benzyl group at nitrogen atom in **2b** increases the Pd–N length [39]. The Pd1/N1/C5–C8 (**2b**) and Pd1/N1/C1–C4 (**2c**) six-membered rings assume half-chair conformations, with atoms N1, C5 and N1, C1 displaced from opposite sides of the mean plane of the remaining four atoms by 0.414(2), 0.496(3) Å and 0.619(2),

Table 1
Crystal data and refinement parameters for complexes **2b**, **2c** and **3c**.

	2b	**2c**	**3c**
Empirical Formula	$C_{39}H_{36}ClNPd$	$C_{37}H_{32}ClNPd$	$C_{43}H_{37}F_3N_2O_3PdS{\cdot}0.5(C_3H_6O)$
Formula weight	660.54	632.49	854.25
T/K	100(1)	100(1)	295 (2)
Crystal system	Triclinic	Monoclinic	Monoclinic
Space group	*P-1*	$P2_1/n$	*C2/c*
a/Å	10.4190(10)	10.0860(10)	22.346 (3)
b/Å	10.9540(11)	17.7680(10)	14.6118 (18)
c/Å	13.8890(12)	16.2960(12)	25.145 (3)
α/°	87.951(10)	90	90
β/°	78.443(10)	95.670(10)	105.6796 (19)
γ/°	82.870(10)	90	90
V/Å^3	1540.9(3)	2906.1(2)	7904.7 (17)
Z	2	4	8
μ (mm^{-1})	0.72	0.757	0.58
D_{cal}/mg m^{-3}	1.424	1.446	1.436
F(000)	680	1296	3504
θ Ranges/°	1.0–35.0	3.05–27.23	7.5–21.6
Independent reflections	4421	6093	7139
Data/restraints/parameters	4421/0/372	6093/0/365	7139/96/518
Goodness-of-fit on F^2	1.100	1.105	1.040
Final R indices	$R_1 = 0.0289$	$R_1 = 0.0230$	$R_1 = 0.0454$
	$wR_2 = 0.0787$	$wR_2 = 0.0590$	$wR_2 = 0.1155$
R indices (all data)	$R_1 = 0.0300$	$R_1 = 0.0235$	$R_1 = 0.0588$
	$wR_2 = 0.0794$	$wR_2 = 0.0593$	$wR_2 = 0.1250$

0.212(2) Å for **2b** and **2c**, respectively. Structure of complex **3c** (Fig. 4) is similar to those of the related complexes **2b** and **2c**, and the new butadienyl fragment (C10, C11, C12, C13) presents a *trans–cis* configuration. Complex **3c** is the second cationic complex of this family structurally characterized by X-ray analysis and all the others are neutral di-inserted complexes [30]. In **3c**, the remarkably tetrahedrally distorted square planar coordination geometry about the Pd metal is provided by two nitrogen atom of the *cis*-arranged pyridine molecule and amine group, the terminal C11 atom of the η^3-butadienyl fragment, and the mid-point of the C8═C9 double bond. The metal is displaced by 0.0246(3) Å from the mean plane through the donor atoms. As observed in **2b** and **2c**, the C10–C11 bond length of the η^2-coordinated alkene unit (1.395(5) Å) was the larger than that of the κ^1-coordinated alkene unit (1.289(5) Å). The η^2-coordinated alkene unit significantly deviates from the planarity [torsion angle C20–C10–C11–C12 = 14.9(6)°]. The Pd–N bond distance involving the N2 nitrogen atom of the pyridine molecule (2.014(3) Å) is remarkably shorter than that involving the N1 atom of the amine group (2.156(3) Å). The six-membered metallacycle (Pd1/N1/C3/C4/C9/C10) assumes a distorted twist boat conformation, as indicated by the puckering parameters $\theta = -115.4(4)°$, $\varphi = -94.0(4)°$ and $Q_T = 0.565(4)$ Å. In the crystal structure, complex cations are linked into a three-dimensional network by N–H···O and C–H···O bonds (Fig. 5) involving the triflate anions and acetone solvent molecules, with H···O separations ranging from 2.11 to 2.50 Å.

2.3. Theoretical approaches

We have attempted to study important aspects of prepared molecules by computational methods. Therefore, the optimization of the structures of four isomers of complexes **3a**, **2b** and **2c** was performed. We named four isomers as *cc*, *ct*, *tt* or *tc*, in which, the first double bond of alkyne attached to the aromatic ring is *cis*, *cis*, *trans* or *trans* and the second one is *cis*, *trans*, *trans* or *cis*. It should be noted that we did not succeed to find a stable geometry with minimum energy for *tt* isomers of each complex. According to the X-ray structures, **3a**, **2b** and **2c** have *tc* geometry, respectively. The calculation of relative Gibbs free energies (Rel G) and enthalpies (Rel H) of three complexes (Table 2) showed that the *tc* isomers are more stable than the others. Calculated ΔG_{cc-tc} for **3a**, **2b** and **2c** are 6.78, 10.39 and 7.05 kcal/mol in the solvent, and also ΔG_{ct-tc} for them are 25.27, 49.25 and 45.25 kcal/mol. As we can see from the calculated relative energies, the stability of the isomers for each complex is as followed: *tc* > *cc* > *ct*. This result is completely in agreement with the proposed mechanism by Ryabov [25] about the insertion of the second alkyne into the palladium–carbon bond of amine palladacycles. According to this mechanism after addition of second alkyne which coordinates in form of *cis*, the resulting *cis*-configuration η^2-coordinated alkenyl fragment will be in the Pd plane. This position is thermodynamically less favorable, therefore, the *cis* → *trans* isomerization of the olefinic fragment takes place, and the η^2-coordinated alkenyl fragment will be perpendicular to the palladium plane. So, the *tc* geometry is more stable structure in such related complexes. In addition, we have been calculated the dipole moment of four complexes. The calculated dipole moments

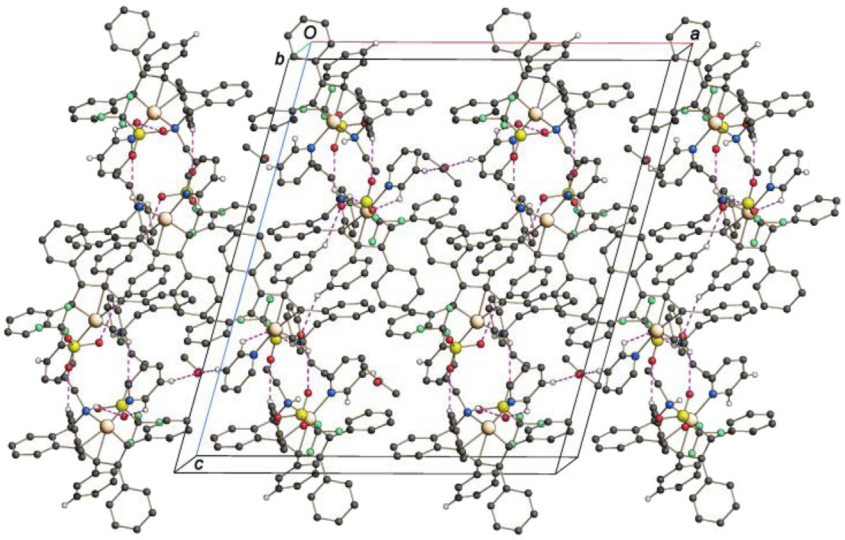

Fig. 5. Crystal packing of **3c** approximately viewed down the *b* axis. Only the major component of the disordered triflate anions are shown. Hydrogen atoms not involved in hydrogen bonding (dashed lines) are omitted.

Table 2
Calculated relative Gibbs free energies and enthalpies of *cc*, *ct* and *tc* isomers of **3a**, **2b** and **2c** and their dipole moments.

Molecule	Rel H (gas phase)	Rel G (gas phase)	Rel G (in solvent)	Dipole moment (Debye)
3a-*cc*	15.07	12.10	7.05	12.50
3a-*ct*	35.78	51.65	45.25	8.34
3a-*tc*	0.00	0.00	0.00	4.84
2b-*cc*	9.27	7.09	6.78	8.65
2b-*ct*	25.76	25.90	25.27	8.56
2b-*tc*	0.00	0.00	0.00	6.66
2c-*cc*	14.28	12.48	10.39	8.62
2c-*ct*	35.69	51.69	49.25	8.70
2c-*tc*	0.00	0.00	0.00	7.36

of **3a**, **2b** and **2c** (with their isomers) are shown in Table 2. As it is shown, the isomer with less dipole moment (*tc* in each complex) is more stable. Also, the dipole moment of the cationic complex **3c** (9.83 Debye) is greater than that of the **3a**-*tc*, **2b**-*tc* and **2c**-*tc*. From the optimized structures of **2b**, **2c** and **3c**, molecular parameters can be obtained. Most important parameters for optimized structures, in comparison with the X-ray parameters, were listed in Table 3. The atom numbering depicted in Fig. 6 for the di-inserted products was used. The comparison between calculated parameters of **2b**-*tc*, **2c**-*tc* and **3c**-*tc* with those in X-ray structures confirms that these structures are closer to the real structures.

We also employed population analyses for *tc* geometric isomers of **3a**, **2b**, **2c** and **3c** to extract the energies of frontier molecular orbitals (FMOs). Graphical presentations of LUMO and HOMO of the structures and their energy gaps (eV) are shown in Fig. 7. In the studied systems the presence of electron-donor groups, Ph, in the η^2-butadienyl moiety decreases the energy of the HOMO. On the contrary, the presence of electron-withdrawing groups, CO_2Me,

Table 3
Selected molecular parameters for calculated isomers (*tc*) in comparison with those in the X-ray structures of **2b**, **2c** and **3c**. Bond lengths are in (Å) and bond angles are in (°).

	2b (*tc*)/X-ray	**2c** (*tc*)/X-ray	**3c** (*tc*)/X-ray
Bond lengths (Å)			
Pd–Cl(N2)	2.504/2.3305(8)	2.446/2.3169(4)	2.283/2.014(3)
Pd–N1	2.225/2.228(3)	2.198/2.1534(14)	2.231/2.156(3)
Pd–C1	2.030/1.997(3)	2.037/2.0111(16)	2.039/1.985(4)
Pd–C3	2.250/2.227(3)	2.254/2.1972(15)	2.271/2.140(3)
Pd–C4	2.280/2.210(3)	2.276/2.2106(16)	2.270/2.189(4)
C1–C2	1.344/1.335(5)	1.347/1.333(2)	1.341/1.289(5)
C2–C3	1.526/1.514(4)	1.526/1.508(2)	1.530/1.504(5)
C3–C4	1.413/1.419(5)	1.412/1.403(2)	1.418/1.395(5)
C4–C5	1.514/1.507(5)	1.515/1.512(2)	1.518/1.514(5)
C5–C6	1.416/1.406(5)	1.417/1.403(2)	1.417/1.396(6)
C6–C7	1.524/1.513(4)	1.519/1.507(2)	1.516/1.507(6)
C7–N	1.505/1.481(4)	1.500/1.477(2)	1.506/1.446(5)
Bond angles (°)			
Cl(N2)–Pd–N	83.35/92.67(7)	83.84/86.77(4)	88.61/91.08(13)
Cl(N2)–Pd–C1	96.03/91.80(9)	99.10/96.64(5)	90.88/92.73(14)
Cl(N2)–Pd–C3	131.06/150.29(8)	150.54/157.34(4)	127.27/66.29(14)
Cl(N2)–Pd–C4	164.62/165.84(8)	173.12/163.39(5)	162.14/87.45(14)
N–Pd–C1	172.09/167.93(11)	171.67/172.02(6)	169.81/169.15(15)
N–Pd–C3	109.29/106.61(11)	108.20/109.74(6)	108.13/107.49(14)
N–Pd–C4	93.58/93.59(11)	92.39/90.25(6)	91.75/92.30(14)
C1–Pd–C3	65.26/65.16(12)	65.63/65.11(6)	64.43/66.29(14)
C1–Pd–C4	84.94/84.63(12)	85.43/88.48(6)	85.65/87.45(14)
Pd–N1–C7	107.89/106.05(19)	108.44/112.67(10)	106.19/112.7(2)
Pd–C1–C2	100.75/48.46(17)	99.82/48.90(9)	102.14/99.3(3)
C1–C2–C3	107.36/106.3(3)	108.37/105.88(14)	106.66/107.8(3)
C2–C3–C4	118.44/117.0(3)	118.72/121.13(14)	117.48/119.8(3)
C3–C4–C5	121.44/122.3(3)	122.43/118.70(14)	121.73/122.7(3)
C4–C5–C6	126.99/125.2(3)	126.71/127.37(14)	126.65/126.3(4)
C5–C6–C7	125.55/124.2(3)	124.42/124.86(14)	124.10/124.6(4)
C6–C7–N	115.50/113.8(3)	112.45/114.54(13)	111.49/114.1(4)

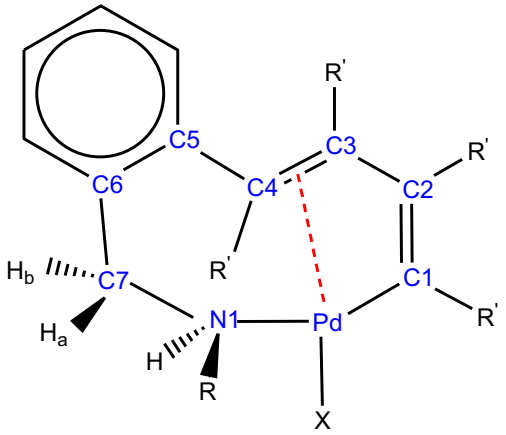

Fig. 6. Numbering scheme adopted for the di-inserted products.

facilitates the oxidation process. The reactivity of the complexes is different and the energy values of 10 frontier orbitals (Table 4) confirm these differences. By comparison between the energies of frontier orbitals, the LUMO–HOMO energy gaps in **3a** and **3c** are less than that in other complexes, which shows these structures are more reactive than **2b** and **2c**. For a more exact determination of the partial atomic charges, NBO calculations were used. The results of these calculations for four complexes (Table 5) showed that the carbon atoms connected to Pd via η^2-bond (C3=C4) in the complexes **2b**, **2c** and **3c** with electron-donor group (Ph), have great negative charges comparing to those in complex **3a** which has electron-withdrawing groups (CO_2Me). Moreover, the Pd atom in the cationic complex **3c** has a greater positive charge in comparison with that in other neutral complexes.

3. Conclusion

In this paper, the synthesis of new mono- and di-inserted palladacycles of secondary benzylamine along with their characterization is reported. Complexes **1a**, **1b** and **1c** react with dimethyl acetylenedicarboxylate and diphenylacetylene producing mono- and di-nuclear palladacycles (**2a**, **3a**, **2b** and **2c**) derived from single and double insertion of the corresponding alkynes into the Pd–C σ bonds. The ^1H and $^{13}C\{^1H\}$ NMR spectra of **2a** and **3a** showed clearly two and four resonances corresponding to methoxy groups in mono- and di-inserted products, respectively. Complex **2c** reacts with $Ag(CF_3SO_3)$ and pyridine to give cationic complex **3c**. The crystal structure of di-inserted complexes **2b**, **2c** and **3c** show the newly formed butadienyl fragments present a *trans–cis* conformation and are η^2–κ^1 coordinated to the palladium(II) center. Theoretical calculations also confirm the greater stability of this conformation for di-inserted products.

4. Experimental

4.1. General

Starting materials and solvents were purchased from Sigma–Aldrich or Alfa Aesar and used without further purification. Infrared spectra were recorded on an FT-IR JASCO 680 spectrophotometer in the spectral range 4000–400 cm^{-1} using the KBr pellets. NMR spectra were measured on a Bruker spectrometer at 400.13 MHz (^1H) and 100.61 MHz (^{13}C) using standard pulse sequences at 298 K. Elemental analysis was performed on Leco, CHNS-932 apparatus.

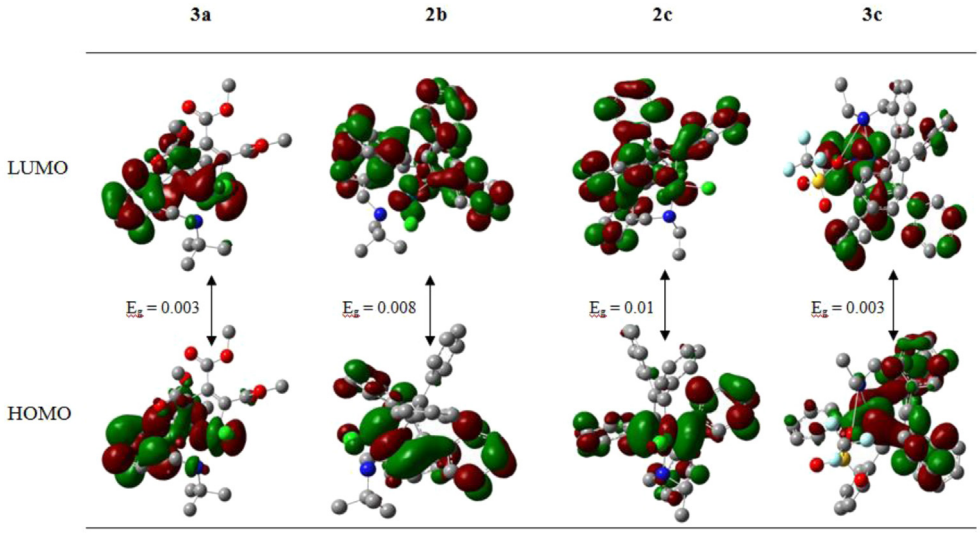

Fig. 7. Graphical presentation of LUMO and HOMO for optimized structures of (*tc*) isomers of **3a**, **2b**, **2c** and **3c** and their energy gaps (eV).

4.2. Synthesis of [Pd_2{(C,N)–$C(CO_2Me)$=$C(CO_2Me)C_6H_4CH_2NH$(t-Bu)}$_2(\mu$-Br)$_2$] (**2a**)

To a solution of palladacycle **1a** (0.040 g, 0.056 mmol) in acetone (15 mL) was added $MeO_2CC{\equiv}CCO_2Me$ (13.7 μL, 0.112 mmol). After 6 h, a yellow solution was formed, which was filtered through a plug of $MgSO_4$. The solvent was removed to ca. 2 mL, and *n*-hexane (15 mL) was added to precipitate **2a** as a yellow solid, which was collected and air-dried. Yield: 70%. IR (KBr, cm^{-1}): ν(NH) = 3228, ν(CO) = 1709, 1628. ^{1}H NMR (DMSO-d_6, ppm): δ = 1.35–1.42 (m, 9H, CH_3), 3.50–3.62 (m, H_a, CH_aH), 3.65, 3.69 (s, 6H, 2OMe), 5.36 (dd, H_b, CH_bH, $^2J_{HH}$ = 11.4 Hz, $^3J_{HH}$ = 4.8 Hz), 4.4 (br, 1H, NH), 7.37–7.50 (m, 3H, C_6H_4), 7.63 (d, 1H, C_6H_4 $^3J_{HH}$ = 6.8 Hz); ^{13}C{^{1}H} NMR (DMSO-d_6, ppm): δ = 29.0, 47.0 (*t*-Bu), 51.0 (OMe), 52.0 (OMe), 57.0 (CH_2), 128.0, 128.4, 131.8, 134.7, 138.4, 138.9 ($C_{aromatic}$), 126.7, 151.6 (C^{α}, C□), 166.3 (CO), 167.1 (CO). Anal. calcd for $C_{34}H_{44}N_2Br_2Pd_2$: C, 42.12; H, 4.57; N, 2.88. Found: C, 42.41; H, 4.58; N, 2.82%.

4.3. Synthesis of [Pd{(C,N)–C(R′)=C(R′)C(R′)=C(R′)} $C_6H_4CH_2NH$(t-Bu)Br] (R′ = CO_2Me) (**3a**)

To a solution of palladacycle **1a** (0.040 g, 0.056 mmol) in acetone (15 mL) was added $MeO_2CC{\equiv}CCO_2Me$ (27.4 μL, 0.224 mmol) and the resulting solution was refluxed for 3 h. A yellow solution was formed which was filtered through a plug of $MgSO_4$. The solvent was removed to ca. 2 mL, and *n*-hexane (15 mL) was added to precipitate **3a** as a yellow solid, which was collected and air-dried. Yield: 68%. IR (KBr, cm^{-1}): ν(NH) = 3250, ν(CO) = 1725, 1713, 1690, 1670. ^{1}H NMR (DMSO-d_6, ppm): δ = 1.46 (m, 9H, CH_3), 3.08 (m, 1H, NH), 3.46, 3.54, 3.65, 3.76 (s, 12H, 4OMe), 4.04 (d, H_a, CH_aH $^2J_{HH}$ = 13.2 Hz), 4.39–4.44 (dd, H_b, CH_bH, $^2J_{HH}$ = 13.2 Hz, $^3J_{HH}$ = 6.0 Hz), 7.03 (d, 1H, C_6H_4), 7.30–7.45 (m, 3H, C_6H_4); ^{13}C{^{1}H} NMR (DMSO-d_6, ppm): δ = 28.5, 49.8 (*t*-Bu), 51.2 (OMe), 51.3 (OMe), 51.8 (OMe), 52.5 (OMe), 59.5 (CH_2), 128.0, 128.1, 129.6, 131.4, 134.5, 134.8 ($C_{aromatic}$), 126.1, 135.3, 143.4, 155.0 (C^{α}, C□, C^{δ}, C□), 157.8 (CO), 165.1 (CO), 168.0 (CO), 171.02 (CO). Anal. calcd for $C_{23}H_{28}NO_8BrPd$: C, 43.65; H, 4.45; N, 2.21. Found: C, 43. 86; H, 4.39; N, 2.16%.

Table 4
The energy values of 10 frontier molecular orbitals (FMOs) of *tc* isomers of **3a**, **2b**, **2c** and **3c**.

Molecule	**3a**-*tc*	**2b**-*tc*	**2c**-*tc*	**3c**
LUMO energy (eV)	−0.121	−0.164	−0.164	−0.165
	−0.148	−0.167	−0.166	−0.168
	−0.156	−0.169	−0.169	−0.168
	−0.165	−0.171	−0.171	−0.170
	−0.170	−0.173	−0.172	−0.176
HOMO energy (eV)	−0.173	−0.181	−0.182	−0.179
	−0.186	−0.192	−0.193	−0.190
	−0.191	−0.208	−0.207	−0.208
	−0.204	−0.230	−0.232	−0.225
	−0.306	−0.293	−0.293	−0.287

4.4. Synthesis of [Pd{(C,N)–C(Ph)=C(Ph)C(Ph)=C(Ph)} $C_6H_4CH_2NH$(t-Bu)Cl] (**2b**)

To a suspension of palladacycle **1b** (0.050 g, 0.082 mmol) in dichloromethane (15 mL) was added PhC≡CPh (0.058 g, 0.327 mmol). After 6 h, a yellow solution was formed, which was filtered through a plug of $MgSO_4$. The solvent was removed to ca. 2 mL, and *n*-hexane (15 mL) was added to precipitate **2b** as a yellow solid, which was collected and air-dried. Yield: 75%. IR (KBr, cm^{-1}): ν(NH) = 3226, ^{1}H NMR ($CDCl_3$, ppm): δ = 1.11 (m, 9H, CH_3), 3.33 (dd, H_a, CH_aH, $^2J_{HH}$ = 12.6 Hz, $^3J_{HH}$ = 3.2 Hz), 3.63 (dd, H_b, CH_bH, $^2J_{HH}$ = 10.2 Hz, $^3J_{HH}$ = 3.2 Hz), 3.91 (br, 1H, NH), 6.81–7.51 (m, 24H, Ph and C_6H_4); ^{13}C{^{1}H} NMR ($CDCl_3$, ppm): δ = 29.5, 48.9 (*t*-Bu), 57.7 (CH_2), 125.3, 125.7, 126.0, 126.4, 126.5, 126.6, 127.4, 127.5, 127.8, 128.9, 129.0, 129.1, 129.3, 129.4, 130.6, 130.8, 130.9, 131.6 ($C_{aromatic}$), 141.6, 135.6, 134.3, 124.8 (C^{α}, C□, C^{δ}, C□). Anal. calcd for $C_{39}H_{36}NClPd$: C, 70.90; H, 5.49; N, 2.12. Found: C, 70.73; H, 5.38; N, 2.10%.

4.5. Synthesis of [Pd{(C,N)–C(Ph)=C(Ph)C(Ph)=C(Ph)} $C_6H_4CH_2NH$(Et)Cl] (**2c**)

To a suspension of palladacycle **1c** (0.050 g, 0.090 mmol) in dichloromethane (15 mL) was added PhC≡CPh (0.064 g, 0.36 mmol). After 6 h, a yellow solution was formed, which was filtered through a plug of $MgSO_4$. The solvent was removed to ca. 2 mL, and *n*-hexane (15 mL) was added to precipitate **2c** as a yellow solid, which was collected and air-dried. Yield: 82%. IR (KBr, cm^{-1}): ν(NH) = 3200, ^{1}H NMR ($CDCl_3$, ppm): δ = 0.98 (t, 3H, CH_3, $^3J_{HH}$ = 7.2 Hz), 1.24 (m, 2H, CH_2), 2.33 (m, H_a, CH_aH), 2.9 (br, 1H, NH), 4.57 (m, H_b, CH_bH), 6.55–7.83 (m, 24H, Ph and C_6H_4); ^{13}C{^{1}H} NMR ($CDCl_3$,

Table 5
The net charge on the atoms around the nine-membered cycle in the di-inserted products; the atom numbering refers to the scheme in Fig. 6.

Molecule	Atom									
	C1	C2	C3	C4	C5	C6	C7	N1	Pd	Cl (N2)
3a-*tc*	−0.124	−0.152	−0.055	−0.079	−0.037	0.0373	−0.321	−0.583	0.348	−0.444
2b-*tc*	−0.113	0.061	−0.207	−0.179	−0.114	0.003	−0.292	−0.596	0.666	−0.476
2c-*tc*	−0.142	0.059	−0.247	−0.219	−0.037	0.002	−0.351	−0.606	0.686	−0.434
3c	−0.152	0.093	−0.285	−0.196	−0.019	0.006	−0.357	−0.649	0.836	−0.736

ppm): $\delta = 12.6, 18.4$ (Et), 48.5 (CH_2), 126.5, 126.6, 126.7, 127.5, 127.8, 127.9, 128.0, 128.2, 128.3, 128.4, 128.5, 128.7, 128.9, 130.6, 130.7, 131.3, 132.6, 132.8 ($C_{aromatic}$), 140.8, 135.8, 132.9, 125.8 (C^{α}, C□, C^{δ}, C□). Anal. calcd for $C_{37}H_{32}NClPd$: C, 70.25; H, 5.09; N, 2.21. Found: C, 70.12; H, 4.96; N, 2.16%.

4.6. Synthesis of [Pd{(C,N)–C(Ph)=C(Ph)C(Ph)=C(Ph)} $C_6H_4CH_2NH(Et)(py)]CF_3SO_3$ (**3c**)

To a solution of complex **2c** (0.030 g, 0.047 mmol) in acetone (15 mL) was added $Ag(CF_3SO_3)$ (0.010 g, 0.047 mmol), and the mixture was stirred for 30 min under light protection and then filtered through a plug of $MgSO_4$ to remove AgCl. Pyridine (3.78 μL, 0.047 mmol) was added to the filtrate, and the resulting yellow solution was stirred for 45 min and then filtered again through $MgSO_4$. The solvent was removed to ca. 2 mL, and *n*-hexane (15 mL) was added to precipitate complex **3c** as a pale yellow solid, which was collected and air-dried. Yield: 80%. IR (KBr, cm^{-1}): $\nu(NH) = 3217$, $\nu(CF_3SO_3) = 1029$, ^1H NMR ($CDCl_3$, ppm): $\delta = 1.65$ (br, 3H, CH_3), 2.19 (m, 2H, CH_2), 3.25 (d, H_a, CH_aH, $^2J_{HH} = 14.4$ Hz), 3.66 (d, H_b, CH_bH, $^2J_{HH} = 14.0$ Hz), 4.54 (br, 1H, NH), 6.15 (d, H_{Ar}, $^3J_{HH} = 7.2$ Hz), 6.87–7.72 (m, 28H, 4Ph + C_6H_4 + $4H_{py}$), 9.48 (d, 1H, *o*-py, $^3J_{HH} = 6.4$ Hz); $^{13}C\{^1H\}$ NMR ($CDCl_3$, ppm): $\delta = 13.15, 30.97$ (Et), 43.75 (CH_2), 125.91, 126.03, 126.12, 126.40, 127.05, 128.12, 128.27, 128.66, 128.84, 128.91, 128.94, 128.98, 129.05, 129.12, 129.27, 129.33, 131.10, 131.41, 131.94, 132.78, 134.41, 135.17, 136.61, 137.30 ($C_{aromatic}$), 151.78, 139.95, 138.82, 124.91 (C^{α}, C□, C^{δ}, C□). Anal. calcd for $C_{37}H_{32}NClPd$: C, 62.58; H, 4.51; N, 3.39. Found: C, 62.41; H, 4.45; N, 3.30%.

4.7. X-ray structure determinations

Single crystals for the X-ray molecular structure determination of **2b**, **2c** and **3c** were obtained by slow evaporation of a solution of **2b** in chloroform/ *n*-hexane and solution of **2c** and **3c** in dichloromethane/ *n*-hexane. The X-ray diffraction experiments for **2b** and **2c** were done at 100 K with the use of Agilent SuperNova single crystal diffractometer (Mo Kα radiation). Analytical numeric absorption correction using a multifaceted crystal model based on expressions derived by R.C. Clark & J.S. Reid was made [55]. Data for **3c** were collected at 295 K on a Bruker APEX-II CCD diffractometer (Mo Kα radiation). Data collection, cell refinement and data reduction were carried out using the APEX2 and SAINT suite of programs [56]. Intensities were corrected for absorption using the program SADABS [56]. The structures were solved by direct methods using the SHELXS97 [57] program for **2b** and **2c** or SIR97 [58] for **3c**, and refined with the use of SHELXL program [57]. Hydrogen atoms were added in the calculated positions and were riding on their respective parent atoms during the refinement. In **3c** the acetone solvent molecule has crystallographically imposed two-fold symmetry, with atoms C44 and O4 lying on the rotation axis. The F and O atoms of the trifluoromethanesulfonate anion were found to be rotationally disordered over two positions (called A and B), with refined site occupancy factors of 0.726(5) and 0.274(5), respectively. During the refinement, the S–O, O···O, C–F and F···F distances were constrained to 1.44(1), 2.42(2), 1.32(1) and 2.15(2) Å, respectively. Moreover the anisotropic displacement parameters of the disordered atoms were restrained to be approximately isotropic and constrained to be equivalent for paired components of the disorder.

4.8. Computational methods

DFT method was applied to optimize all structures and calculate molecular and spectral parameters of prepared compounds in the gas phase. The energy values in the solvent (dichloromethane) were calculated using SCRF keyword with Tomasi's polarized continuum (PCM) model [59]. Gaussian 09 program package [60] was employed for optimizing the structures and calculation of molecular properties. To perform DFT calculations, Becke's three-parameter exchange functional [61] was used in combination with the Lee–Yang–Parr correlation functional (B3LYP) with LANL2DZ basis set [62]. All molecules have been used without any symmetry restriction and C1 symmetry was assumed for all molecules. NBO analyses [63] were carried out as implemented in the Gaussian program package using B3LYP/LANL2DZ level of theory.

Acknowledgments

We are grateful for the financial support from the Department of Chemistry, Isfahan University of Technology (IUT).

Appendix A. Supplementary material

CCDC 924332, 924333 and 945922 contain the supplementary crystallographic data for this paper. These data can be obtained free of charge from The Cambridge Crystallographic Data Centre via www.ccdc.cam.ac.uk/data_request/cif.

References

[1] A. Bahsoun, J. Dehand, M. Pfeffer, M. Zinsius, S.E. Bouaoud, G. Le Borgne, Dalton Trans. (1979) 547–556.
[2] F. Maassarani, M. Pfeffer, G. Le Borgne, Organometallics 6 (1987) 2029–2043.
[3] H. Ossor, M. Pfeffer, J.T.B.H. Jastrzebski, C.H. Stam, Inorg. Chem. 26 (1987) 1169–1171.
[4] M. Pfeffer, M.A. Rotteweel, J.P. Sutter, A. De Cian, J. Fischer, J. Organomet. Chem. 371 (1989) C21–C25.
[5] G.Z. Wu, A.L. Rheingold, R.F. Heck, Organometallics 6 (1987) 2386–2391.
[6] J. Dupont, M. Pfeffer, M.A. Rotteveel, A. De Cian, J. Fischer, Organometallics 8 (1989) 1116–1118.
[7] W. Tao, L.J. Silverberg, A.L. Rheingold, R.F. Heck, Organometallics 8 (1989) 2550–2559.
[8] M. Pfeffer, Pure Appl. Chem. 64 (1992) 335–342.
[9] N. Beydoun, M. Pfeffer, Synthesis (1990) 729–731.
[10] J. Spencer, M. Pfeffer, Tetrahedron Asymmetry 6 (1995) 419–426.
[11] M. Pfeffer, N. Sutter-Beydoun, A. De Cian, J. Fischer, J. Organomet. Chem. 453 (1993).
[12] M. Pfeffer, M.A. Rotteveel, G. Le Borgne, J. Fischer, J. Org. Chem. 57 (1992) 2147–2154.
[13] M. Pfeffer, J.P. Sutter, M.A. Rotteveel, A. De Cian, J. Fischer, Tetrahedron 48 (1992) 2427–2440.
[14] J. Dupont, M. Pfeffer, L. Theurel, M.A. Rotteveel, A. De Cian, J. Fisher, New J. Chem. 15 (1991) 551–558.
[15] N. Beydoun, M. Pfeffer, A. De Cian, J. Fisher, Organometallics 10 (1991) 3693–3697.

[16] M. Pfeffer, J.P. Sutter, A. De Cian, J. Fischer, Organometallics 12 (1993) 1167–1173.
[17] J. Vicente, I. Saura-Llamas, C. Grunwald, C. Alcaraz, P.G. Jones, D. Bautista, Organometallics 21 (2002) 3587–3595.
[18] J. Vicente, J.A. Abad, J. Gil-Rubio, P.G. Jones, Organometallics 14 (1995) 2677–2688.
[19] J. Vicente, J.A. Abad, J. Gil-Rubio, J. Organomet. Chem. 436 (1992) C9–C12.
[20] J. Vicente, J.A. Abad, J. Lopez-Serrano, P.G. Jones, C. Najera, L. Botella-Segura, Organometallics 24 (2005) 5044–5057.
[21] J. Spencer, M. Pfeffer, Adv. Met. Org. Chem. 6 (1998) 103–144.
[22] M. Pfeffer, Recl. Trav. Chim. Pays-Bas 109 (1990) 567–576.
[23] A.D. Ryabov, Synthesis (1985) 233–252.
[24] J. Albert, J. Granell, A. Luque, M. Font-Bardia, X. Solans, Polyhedron 25 (2006) 793–800.
[25] A.D. Ryabov, R. van Eldik, G. Le Borgne, M. Pfeffer, Organometallics 12 (1993) 1386–1393.
[26] V. Montoya, J. Pons, J. Garcıa-Anton, X. Solans, M. Font-Bardia, J. Ros, Organometallics 26 (2007) 3183–3190.
[27] J. Dupont, M. Pfeffer (Eds.), Palladacycles: Synthesis, Characterization and Application, Wiley-VCH, Weinheim, Germany, 2008.
[28] J. Vicente, I. Saura-Llamas, M.G. Palin, P.G. Jones, Dalton Trans. (1995) 2535–2539.
[29] J. Vicente, I. Saura-Llamas, M.C. Ramírez de Arellano, Dalton Trans. (1995) 2529–2533.
[30] J. Vicente, I. Saura-Llamas, J. Turpin, M.C. Ramírez de Arellano, Organometallics 18 (1999) 2683–2693.
[31] I. Omae, Coord. Chem. Rev. 248 (2004) 995–1023.
[32] J. Albert, L. D'Andrea, J. Granell, J. Zafrilla, M. Font-Bardia, X. Solans, J. Organomet. Chem. 692 (2007) 4895–4902.
[33] J. Albert, L. D'Andrea, G. Garcia, J. Granell, A. Rahmouni, M. Font-Bardia, T. Calvet, Polyhedron 28 (2009) 2559–2564.
[34] J. Vicente, I. Saura-Llamas, J. Turpin, D. Bautista, C.R. De Arellano, P.G. Jones, Organometallics 28 (2009) 4175–4195.
[35] J. Vicente, I. Saura-Llamas, J.A. Garcia-Lopez, D. Bautista, Organometallics 29 (2010) 4320–4338.
[36] J.A. Garcıa-Lopez, M.J. Oliva-Madrid, I. Saura-Llamas, D. Bautista, J. Vicente, Chem. Commun. 48 (2012) 6744–6746.
[37] J.A. Garcıa-Lopez, M.J. Oliva-Madrid, I. Saura-Llamas, D. Bautista, J. Vicente, Organometallics 32 (2013) 1094–1105.
[38] J. Vicente, I. Saura-Llamas, Comments Inorg. Chem. 28 (2007) 39–72 and references therein.
[39] K. Karami, M. Hosseini Kharat, C. Rizzoli, J. Lipkowski, J. Organomet. Chem. 728 (2013) 16–22.
[40] K. Karami, M. Hosseini-Kharat, H. Sadeghi-Aliabadi, J. Lipkowski, M. Mirian, Polyhedron 50 (2012) 187–192.
[41] C. Lopez, S. Perez, X. Solans, M. Font-Bardia, J. Organomet. Chem. 690 (2005) 228–243.
[42] D.H. Johnston, D.F. Shriver, Inorg. Chem. 32 (1993) 1045–1047.
[43] P.J. Riedel, N. Arulsamy, M.P. Mehn, Inorg. Chem. Commun. 14 (2011) 734–737.
[44] A.J. Godo, A.C. Benyei, B. Duff, D.A. Egan, P. Buglyo, RSC Adv. 2 (2012) 1486–1495.
[45] G. Zhao, Q.G. Wang, T.C.W. Mak, Tetrahedron Asymmetry 9 (1998) 2253–2257.
[46] G. Zhao, Q.G. Wang, T.C.W. Mak, J. Organomet. Chem. 574 (1999) 311–317.
[47] R.B. Bedford, C.S.J. Cazin, S.J. Coles, T. Gelbrich, P.N. Horton, M.B. Hursthouse, M.E. Light, Organometallics 22 (2003) 987–999.
[48] A. Fernandez, D. Vazquez-Garcia, J.J. Fernandez, M. Lopez-Torres, A. Suarez, S. Castro-Juiz, J.M. Vila, Eur. J. Inorg. Chem (2002) 2389–2401.
[49] J. Albert, J. Granell, J. Zafrilla, M. Font-Bardia, X. Solans, J. Organomet. Chem. 690 (2005) 422–429.
[50] J.M. Chitanda, J. Wilson Quail, S.R. Foley, J. Organomet. Chem. 694 (2009) 1542–1548.
[51] T.G. Appleton, H.C. Clark, L.E. Manzer, Coord. Chem. Rev. 10 (1973) 335–422.
[52] G. Zhao, Q.C. Yang, T.C.W. Mak, Organometallics 18 (1999) 3623–3636.
[53] M. Benito, C. Lopez, X. Morvan, X. Solans, M. Font-Bardia, Dalton Trans. (2000) 4470–4478.
[54] S. Perez, C. Lopez, A. Caubet, A. Pawelczyk, X. Solans, M. Font-Bardia, Organometallics 22 (2003) 2396–2408.
[55] R.C. Clark, J.S. Reid, Acta Crystallogr. A51 (1995) 887–897.
[56] Bruker, APEX2 (Version 2008.1–0), SAINT (Version 7.51A) and SADABS (Version 2007/4), Bruker AXS Inc., Madison, Wisconsin, USA, 2008.
[57] G.M. Sheldrick, Acta Crystallogr. A 64 (2008) 112–122.
[58] A. Altomare, M.C. Burla, M. Camalli, G. Cascarano, C. Giacovazzo, A. Guagliardi, A.G.G. Moliterni, G. Polidori, R. Spagna, J. Appl. Crystallogr. 32 (1999) 115–119.
[59] S. Mietrus, J. Tomasi, Chem. Phys. 65 (1982) 239–245.
[60] M.J. Frisch, G.W. Trucks, H.B. Schlegel, G.E. Scuseria, M.A. Robb, J.R. Cheeseman, G. Scalmani, V. Barone, B. Mennucci, G.A. Petersson, H. Nakatsuji, M. Caricato, X. Li, H.P. Hratchian, J. Izmaylov, A.F. Bloino, G. Zheng, J.L. Sonnenberg, M. Hada, M. Ehara, K. Toyota, R. Fukuda, J. Hasegawa, M. Ishida, T. Nakajima, Y. Honda, O. Kitao, H. Nakai, T. Vreven, J.A. Montgomery, J.E. Peralta, F. Ogliaro, M. Bearpark, J.J. Heyd, E.K.N. Brothers, V.N. Staroverov, R. Kobayashi, J. Normand, K. Raghavachari, A. Rendell, J.C. Burant, S.S. Iyengar, J. Tomasi, M. Cossi, N. Rega, J.M. Millam, M. Klene, J.E. Knox, J.B. Cross, V. Bakken, C. Adamo, J. Jaramillo, R. Gomperts, R.E. Stratmann, O. Yazyev, A.J. Austin, R. Cammi, C. Pomelli, J.W. Ochterski, R.L. Martin, K. Morokuma, V.G. Zakrzewski, G.A. Voth, P. Salvador, J.J. Dannenberg, S. Dapprich, A.D. Daniels, O. Farkas, J.B. Foresman, J.V. Ortiz, J. Cioslowski, D.J. Fox, Gaussian, Inc., Wallingford CT, 2009.
[61] A.D. Becke, J. Chem. Phys. 98 (1993) 5648–5652.
[62] C.T. Lee, W.T. Yang, R.G. Parr, Phys. Rev. B 37 (1988) 785–789.
[63] E.D. Glendening, A.E. Reed, J.E. Carpenter, F. Weinhold, NBO Version 3.1.